Pyridyl Pyrrolide Boron Complexes: The Facile Generation of Thermally Activated Delayed Fluorescence and Preparation of Organic Light-Emitting Diodes

Yi-Jiun Shiu[+], Yung-Chen Cheng[+], Wei-Lung Tsai, Chung-Chih Wu,* Chun-Tien Chao, Chin-Wei Lu, Yun Chi,* Yi-Ting Chen, Shih-Hung Liu, and Pi-Tai Chou*
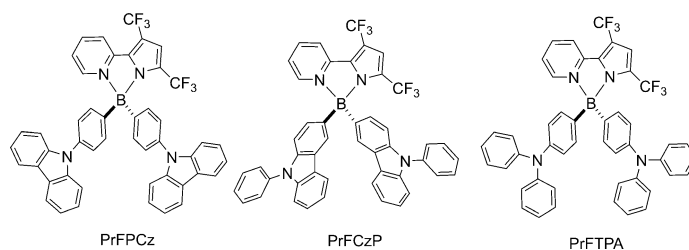
Abstract: *The electron positive boron atom usually does not contribute to the frontier orbitals for several lower-lying electronic transitions, and thus is ideal to serve as a hub for the spiro linker of light-emitting molecules, such that the electron donor (HOMO) and acceptor (LUMO) moieties can be spatially separated with orthogonal orientation. On this basis, we prepared a series of novel boron complexes bearing electron deficient pyridyl pyrrolide and electron donating phenylcarbazolyl fragments or triphenylamine. The new boron complexes show strong solvent-polarity dependent charge-transfer emission accompanied by a small, non-negligible normal emission. The slim orbital overlap between HOMO and LUMO and hence the lack of electron correlation lead to a significant reduction of the energy gap between the lowest lying singlet and triplet excited states ($\Delta E_{T\text{-}S}$) and thereby the generation of thermally activated delay fluorescence (TADF).*

Organic light-emitting diodes (OLEDs) have rapidly progressed since the first report of electroluminescence (EL) using organic fluorophore by Tang and VanSlyke in 1987.[1] Important advancements were then made possible through the utilization of precious-metal-based phosphors, resulting in an increase of internal EL quantum efficiencies (η_{int}) from 25% to 100%.[2] However, the issue of costs becomes a major obstacle for these phosphors. One promising approach is to employ a metal-free luminophore that shows efficient thermally activated delayed-fluorescence (TADF).[3] It is believed that, by controlling the spatial overlap between the highest occupied molecular orbital (HOMO) and the lowest unoccupied molecular orbital (LUMO), the energy gap ($\Delta E_{T\text{-}S}$)

between the lowest energy singlet (S_1) and triplet (T_1) states can be effectively reduced.[4]

This tactic not only promotes the singlet–triplet mixing, but also facilitates the reverse intersystem crossing from T_1 to S_1 and hence harvesting the delayed fluorescence via thermal activation.[5] As a result, numerous systems that displayed notable TADF behaviors have been investigated, the associated electron transfer properties can be categorized being intra- and intermolecular type of donor–acceptor composites; the intermolecular type is ascribed to the exciplex formation.[6] However, despite the difference in mechanism the similarity lies in that most of them rely on the hydrocarbon-based core structure. In an aim to expand the versatility and applicability, there is a great demand for TADF materials with a different molecular design. We report herein a new approach to the TADF emitters. The boron-containing fragment was chosen for its high rigidity and good electron-accepting ability,[7] which then serves as a hub for anchoring both the donor and acceptor groups without affecting their electronic properties. Consequently, under solution-processed conditions,[8] we demonstrate for the first time the boron-complex-based OLEDs, these give external EL quantum efficiencies (η_{ext}) of 13.6%, a result attributed to the TADF characteristics.

These organoboron compounds inherited the traditional designs of pyrazolate- and pyrrolide-substituted boron complexes,[9] except for incorporation of electron-donating triphenylamine or carbazolyl fragments.[10] Their syntheses started with the isolation of an air-stable intermediate PrFBCl$_2$, PrFH = 2-(3,5-bis(trifluoromethyl)-1*H*-pyrrol-2-yl)pyridine. Subsequently, treatment of PrFBCl$_2$ with the in situ generated Grignard regent and in presence of CuI[11] afforded the products PrFPCz, PrFCzP, and PrFTPA (Scheme 1). This synthetic methodology is different from that described for the typical BPh$_2$ and BAr$_2$ derivatives,

[*] Y.-J. Shiu,[+] W.-L. Tsai, Prof. C.-C. Wu
Graduate Institute of Electronics Engineering and Department of Electrical Engineering, National Taiwan University
Taipei 10617 (Taiwan)
E-mail: wucc@ntu.edu.tw

Y.-C. Cheng,[+] C.-T. Chao, Dr. C.-W. Lu, Prof. Y. Chi
Department of Chemistry, National Tsing Hua University
Hsinchu 30013 (Taiwan)
E-mail: ychi@mx.nthu.edu.tw

Y.-T. Chen, Dr. S.-H. Liu, Prof. P.-T. Chou
Department of Chemistry, National Taiwan University
Taipei 10617 (Taiwan)
E-mail: chop@ntu.edu.tw

[+] These authors contributed equally to this work.

Supporting information for this article is available on the WWW under http://dx.doi.org/10.1002/anie.201509231.

Scheme 1. Structural drawings of the boron complexes, PrFPCz, PrFCzP, and PrFTPA.

which involves the direct treatment of PrFH and analogues with BPh$_3$ or with BFAr$_2$, owing to the inaccessibility of corresponding diaryl or triaryl boron reagents.[12]

The UV/Vis absorption and emission spectra of the new boron complexes in different solvents at room temperature are shown in Figure 1, while pertinent photophysical data are listed in Table 1. As can be seen, the lower energy absorption peaks for these complexes at about 350 nm have a large molar extinction coefficient in the order of around 1.5×10^4 M^{-1} cm^{-1} (in toluene). Thus, this characteristic absorption can reasonably be assigned to a ligand-centered π–π* transition, which is independent of solvent polarity. Furthermore, all these
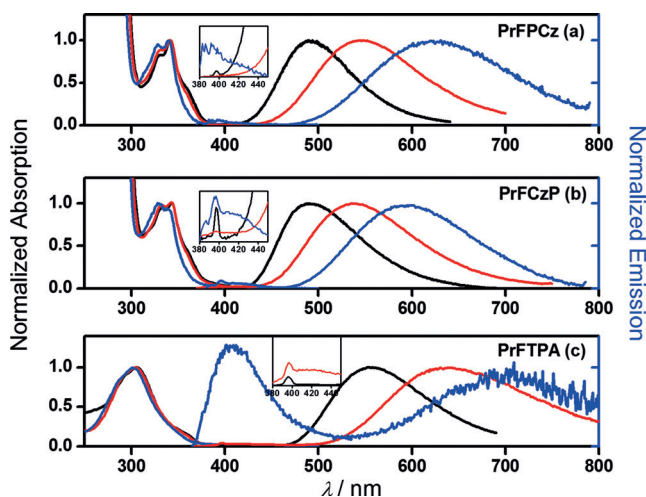

Figure 1. Absorption and emission spectra of a) PrFPCz, b) PrFCzP, and c) PrFTPA in toluene (black), CH$_2$Cl$_2$ (red), and acetonitrile (blue) at 298 K. Inset: The 10x enlargement of emission from 380 to 450 nm. Note that the appearance of a sharp peak at approximately 396 nm is ascribed to the Raman peak (C–H vibration) of the solvent upon 355 nm excitation.

Table 1: Selected photophysical properties of the complexes in toluene and acetonitrile at room temperature.

Compound (solvent)	LE [nm]	CT [nm]	PLQY [%]	Lifetime[b]	
				τ_{LE} [ns]	τ_{CT} [ns] (pre-exp factor)
PrFPCz (toluene)		485	9.3,[a] 22.5[b]		27.5 (–)
PrFPCz (CH$_3$CN)	390	620		0.4	4.9 (–)
PrFCzP (toluene)		495	7.4,[a] 23.4[b]		31.1 (0.9970) 16045 (0.0030)
PrFCzP (CH$_3$CN)	410	600		6.1	8.0 (–)
PrFTPA (toluene)		560	10.9,[a] 40.8[b]		63.1 (0.9945) 4240 (0.0055)
PrFTPA (CH$_3$CN)	410	705		2.7	1.4 (–)

[a] measured in aerated solution. [b] measured in degassed solution.

complexes exhibit structureless emission in the visible range, of which the peak wavelength is strongly solvent dependent, being red shifted upon increasing the solvent polarity. For example, the emission maximum of PrFPCz occurs at 485 nm (in toluene), 550 nm (in CH$_2$Cl$_2$), and 620 nm (in CH$_3$CN), which can be ascribed to the inter-ligand charge-transfer (CT) transition (see below), resulting in a large change of dipole moment in the electronically excited state versus that of the ground state, which is conventionally termed solvatochromism.[13] Similar behavior was observed for PrFCzP and PrFTPA. It is worth of noting that a non-negligible band at approximately 390–410 nm for PrFPCz and PrFCzP, and became more prominent for PrFTPA in CH$_3$CN owing to its very weak CT emission. This short-wavelength emission is defined as the localized-excitation (LE) emission to distinguish it from the CT emission. This phenomenon is reminiscent of a number of compounds that exhibit twisted intramolecular charge transfer (TICT).[15] Similar dual emission has been observed recently by Adachi and co-workers on the dihydrophenazine-based emitters exhibiting TADF.[16] Since the contribution of localized-excitation emission is very minor and becomes negligible in the solid state (see below), relevant discussion is elaborated in the Supporting Information.

The time-dependent density functional theory (TD-DFT) calculations were then performed to gain insight into the basic photophysical data. All pertinent assignments of the lowest lying singlet S$_0$→S$_1$ absorption transitions are listed in Table S3 and Figure S2 in the Supporting Information, while Figure 2 depicts the HOMO and LUMO of PrFTPA as representative example. Analyses conclude that the lowest energy transition is HOMO→LUMO in nature, in which the electron density distribution of HOMO and LUMO is mainly localized at triphenylamine and the chelating pyridyl pyrrolide, respectively, for PrFTPA. Therefore, the S$_0$→S$_1$ transition for all the new complexes are assigned to the inter-ligand charge transfer, in which HOMO and LUMO are spatially separated by the boron atom. The electron-density contribution of boron in both HOMO and LUMO for PrFTPA is negligible, being 0.40 % and 0.48 %, respectively. Accordingly, the S$_0$→S$_1$ transition reveals a large charge-transfer character, for which the transition moment in terms of oscillator strength is virtually zero, that is, a forbidden transition (see Table S3).[14]

The photoluminescence quantum yields (PLQY) of the major CT emission for PrFPCz, PrFCzP, and PrFTPA in degassed toluene are recorded to be 22.5, 23.4, and 40.8 %,
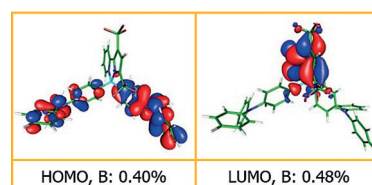

Figure 2. The frontier orbitals of PrFTPA. "B" indicates the relative electron density at boron atom. Energy levels calculated from redox potentials and (DFT studies): HOMO = 5.14 (4.90) eV and LUMO = 2.78 (2.60) eV.

respectively (Table 1). Furthermore, the lifetime of PrFPCz shows only a single exponential decay component (27.5 ns) in toluene, while that of PrFCzP and PrFTPA clearly reveals two single exponential decay components, consisting of a fast decay with a lifetime of 31 ns (for PrFCzP) and 63 ns (PrFTPA) and a slow decay with a lifetime of 16 μs (PrFCzP) and 4.2 μs (PrFTPA; see Figure S3 and Table 1). Both the short and long decay components are subject to oxygen quenching. We thus conclude that the short and long decay components are ascribed to the prompt fluorescence and TADF, the TADF originates from thermal equilibrium at room temperature between the S_1 and the T_1 state, and the difference in energy $\Delta E_{T\text{-}S}$ (defined as T_1 minus S_1) is derived as follows [Eq. (1)]:[17]

$$[I]_t = I_0 \left\{ \frac{k_{\text{isc}}}{k_{\text{isc}} + k_{\text{risc}}} e^{-t/\tau_1} + \frac{k_{\text{risc}}}{k_{\text{isc}} + k_{\text{risc}}} e^{-t/\tau_2} \right\} \qquad (1)$$

where I_0 is a proportional constant incorporating both radiative decay rate constant of the CT emission and instrument factor, τ_1 and τ_2 are the observed lifetime of the fast and slow decay components. As a result, the equilibrium constant $K_{eq} = k_{\text{isc}}/k_{\text{risc}}$ can be obtained by the ratio of the pre-exponential factor (at $t = 0$; see Table 1) in Equation (1), which is deduced to be 332 (PrFCzP) and 181 (PrFTPA) in degassed toluene. According to the $\Delta E_{T\text{-}S} - K_{eq}$ relationship expressed as $\Delta E_{T\text{-}S} = -RT \ln(K_{eq}/3)$ where a factor of 3 stands for the triplet degenerate states, $\Delta E_{T\text{-}S}$ is then deduced to be -2.8 and -2.4 kcal mol^{-1} for PrFCzP and PrFTPA in toluene, respectively. TADF was not observed for PrFPCz in toluene (see above) and other polar solvents. This is perhaps due to the larger solvent polarity stabilization of the triplet state (T_1) than the singlet state (S_1), resulting in a large negative $\Delta E_{T\text{-}S}$ for PrFPCz such that $T_1 \rightarrow S_1$ reverse intersystem is thermodynamically unfavorable. Nevertheless, as elaborated below, TADF for all the new boron complexes is evident in the solid film, which contributes greatly to OLEDs.

Spectroscopic measurement of the boron complexes in the solid film has also been performed. Figure S4 a depicts the fluorescent spectra (measured at room temperature) and phosphorescent spectra (measured at 77 K) of PrFPCz, PrFCzP, and PrFTPA doped (with a doping concentration of 8 wt %) in a large-triplet-energy host TCTA [(4,4′,4′′-tri(N-carbazolyl)triphenylamine)].[18] The fluorescence and phosphorescence of PrFPCz, PrFCzP, and PrFTPA in doped films give broad and structureless spectra peaking around 522 nm, 518 nm for PrFPCz, 505 nm, 491 nm for PrFCzP, and 520 nm, 531 nm for PrFTPA , respectively (Table S4). From the difference in the onset wavelengths of fluorescence and phosphorescence spectra, relatively small triplet-to-singlet energy gaps $\Delta E_{T\text{-}S}$ of approximately -57 meV (-1.3 kcal mol^{-1}), -65 meV (-1.5 kcal mol^{-1}), and -38 meV (-0.9 kcal mol^{-1}) are extracted for PrFPCz, PrFCzP, and PrFTPA, respectively, indicating the possibility of TADF in these boron complexes doped in solid films as well. Indeed, the transient photoluminescence (PL; Figure S4 b) of PrFPCz, PrFCzP, and PrFTPA in the TCTA host

measured by monitoring the intensity of the PL peak wavelength at room temperature clearly exhibits a delayed component (with a lifetime of 4.3 μs, 2.4 μs, and 3.1 μs, respectively, Table S4) following a prompt component (with a lifetime of 143 ns, 33 ns, and 40 ns, respectively), confirming their distinct TADF characteristics in doped films. Intriguingly, while distinct TADF is not readily observed for PrFPCz in polar solvents, it exhibits clear TADF characteristics in doped films. At room temperature, PrFPCz, PrFCzP, and PrFTPA doped in TCTA exhibit a PLQY of approximately 40 %, 38 %, and 60 %, respectively. Noticeably, PrFTPA doped in TCTA exhibits a significantly higher PLQY of about 60 % than the others at room temperature.

The TADF emitters PrFPCz, PrFCzP, and PrFTPA were further subjected to electroluminescence (EL) studies. The devices had the structure: glass substrate/ITO anode/PEDOT:PSS (30 nm)/TCTA: 8 wt % PrFPCz, PrFCzP, or PrFTPA (40 nm)/3TPYMB (50 nm)/LiF (0.6 nm)/Al (100 nm). The transparent poly(3,4-ethylenedioxythiophene): poly(styrenesulfonate) (PEDOT:PSS) served as the hole-injection layer.[19] TCTA with a large-triplet-energy was employed as the hole-transport and host material.[19] Tris-[3-(3-pyridyl)mesityl]borane (3TPYMB),[20] LiF and Al acted as the electron-transport layer, electron injection layer and the cathode, respectively. Figure 3 a shows the device configuration and chemical structures of materials used in this work.

Figure 3 b–d shows the EL characteristics of all studied devices, while data are summarized in Table 2. The EL spectra (Figure 3 b) of all the devices are similar to their corresponding PL spectra in doped films (i.e., blue-green to green emission and more red-shift EL for the PrFPCz and PrFTPA devices), indicating pure EL from either PrFPCz, PrFCzP, or PrFTPA. All devices exhibit similar $I\text{–}V$ characteristics (Figure 3 c), with a low turn-on voltage of about 2–2.5 V (defined as the voltage when the luminance becomes detectable) and low operation voltage (e.g. ca. 3–4 V for a practical brightness
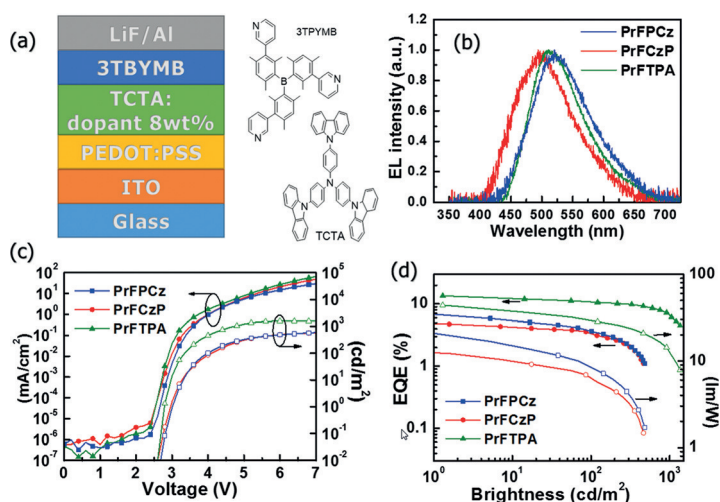

Figure 3. a) The device configuration and chemical structures of materials used in this work. b) EL spectra, c) current–voltage-luminance (*I–V–L*) characteristics, and d) external quantum efficiency and power efficiency of PrFPCz, PrFCzP, and PrFTPA devices.

Table 2: The electroluminescence parameters of PrFPCz, PrFCzP and PrFTPA.

Device		EQE [%]	Current efficiency [cd A^{-1}]	Power efficiency [lm W^{-1}]
PrFPCz	Peak	7.6	22.2	24.9
	100 cd m^{-2}	3.6	10.6	8.32
PrFCzP	Peak	4.8	11.8	13.3
	100 cd m^{-2}	3.1	7.7	5.7
PrFTPA	Peak	13.5	39.2	43.9
	100 cd m^{-2}	10.6	30.8	28.4

of 100 cd m^{-2}). As shown in Figure 3 d (and Table 2), the PrFTPA device gives significantly higher external quantum efficiency (EQE), current efficiency, and power efficiency up to 13.5%, 39.2 cd A^{-1}, 43.9 lm W^{-1} versus 7.6%, 22.2 cd A^{-1}, 24.9 lm W^{-1} for the PrFPCz device and 4.8%, 11.8 cd A^{-1}, 13.3 lm W^{-1} for the PrFCzP device. It is not surprising that the PrFTPA device shows highest EL efficiencies among all devices, since PrFTPA possesses the highest PLQY. Yet, a maximal EQE of over 10% is certainly beyond the theoretical limit of a normal fluorescent emitter with a PLQY of 60%. Considering the PLQY of 60%, a singlet ratio around 25% in EL for normal fluorescent emitters, and an optical out-coupling efficiency of 20–25% for typical OLEDs, an upper limit of EQE of only about 4% would be expected. The observation of a > 10% EQE clearly indicates effective recycling and utilization of the triplet excitons formed during the EL process, through the effective TADF (or reverse intersystem crossing) process of PrFTPA, as already indicated by its delayed fluorescence in PL. Similarly, although lower EQE is observed for PrFPCz and PrFCzP devices, yet their efficiencies are also significantly beyond those expected from normal fluorescent emitters with the observed PLQYs, again indicating harvesting of triplet excitons for EL through TADF.

In conclusion, we exploit the boron atom as a hub to anchor both electron-donating and electron-accepting moieties, for which the poor orbital overlap between donor and acceptor provide the needed criteria for reduced $\Delta E_{T\text{-}S}$. Moreover, all of the resulting complexes show intense luminescence accompanied by prominent TADF. Among all studied OLEDs, the device using PrFTPA processed by spin coating achieved EQE of 13.5%. The results demonstrate for the first time that boron complexes can be used as a core composite to attain high performance OLEDs via harvesting TADF, broadening the horizon of the TADF class of molecules.

Acknowledgements

[1] C. W. Tang, S. A. VanSlyke, *Appl. Phys. Lett.* **1987**, *51*, 913.

[2] a) M. A. Baldo, D. F. O'Brien, Y. You, A. Shoustikov, S. Sibley, M. E. Thompson, S. R. Forrest, *Nature* **1998**, *395*, 151; b) S. Lamansky, P. Djurovich, D. Murphy, F. Abdel-Razzaq, H.-E. Lee, C. Adachi, P. E. Burrows, S. R. Forrest, M. E. Thompson, *J. Am. Chem. Soc.* **2001**, *123*, 4304; c) A. B. Tamayo, B. D. Alleyne, P. I. Djurovich, S. Lamansky, I. Tsyba, N. N. Ho, R. Bau, M. E. Thompson, *J. Am. Chem. Soc.* **2003**, *125*, 7377.

[3] a) H. Uoyama, K. Goushi, K. Shizu, H. Nomura, C. Adachi, *Nature* **2012**, *492*, 234–238; b) C. Adachi, *Jpn. J. Appl. Phys.* **2014**, *53*, 060101; c) H. Nakanotani, T. Higuchi, T. Furukawa, K. Masui, K. Morimoto, M. Numata, H. Tanaka, Y. Sagara, T. Yasuda, C. Adachi, *Nat. Commun.* **2014**, *5*, 4016; d) Y. Tao, K. Yuan, T. Chen, P. Xu, H. Li, R. Chen, C. Zheng, L. Zhang, W. Huang, *Adv. Mater.* **2014**, *26*, 7931–7958; e) K. Shizu, M. Uejima, H. Nomura, T. Sato, K. Tanaka, H. Kaji, C. Adachi, *Phys. Rev. Appl.* **2015**, *3*, 014001.

[4] a) K. Goushi, K. Yoshida, K. Sato, C. Adachi, *Nat. Photonics* **2012**, *6*, 253–258; b) V. Jankus, P. Data, D. Graves, C. McGuinness, J. Santos, M. R. Bryce, F. B. Dias, A. P. Monkman, *Adv. Funct. Mater.* **2014**, *24*, 6178–6186; c) S. Hirata, Y. Sakai, K. Masui, H. Tanaka, S. Y. Lee, H. Nomura, N. Nakamura, M. Yasumatsu, H. Nakanotani, Q. Zhang, K. Shizu, H. Miyazaki, C. Adachi, *Nat. Mater.* **2015**, *14*, 330–336.

[5] A. Endo, K. Sato, K. Yoshimura, T. Kai, A. Kawada, H. Miyazaki, C. Adachi, *Appl. Phys. Lett.* **2011**, *98*, 083302.

[6] a) D. Graves, V. Jankus, F. B. Dias, A. Monkman, *Adv. Funct. Mater.* **2014**, *24*, 2343–2351; b) B. S. Kim, J. Y. Lee, *Adv. Funct. Mater.* **2014**, *24*, 3970–3977; c) W.-Y. Hung, G.-C. Fang, S.-W. Lin, S.-H. Cheng, K.-T. Wong, T.-Y. Kuo, P.-T. Chou, *Sci. Rep.* **2014**, *4*, 5161; d) C. Fan, C. Duan, Y. Wei, D. Ding, H. Xu, W. Huang, *Chem. Mater.* **2015**, *27*, 5131–5140.

[7] Y. Kitamoto, T. Namikawa, D. Ikemizu, Y. Miyata, T. Suzuki, H. Kita, T. Sato, S. Oi, *J. Mater. Chem. C* **2015**, *3*, 9122–9130.

[8] L. Mei, J. Hu, X. Cao, F. Wang, C. Zheng, Y. Tao, X. Zhang, W. Huang, *Chem. Commun.* **2015**, *51*, 13024–13027.

[9] a) C.-C. Cheng, W.-S. Yu, P.-T. Chou, S.-M. Peng, G.-H. Lee, P.-C. Wu, Y.-H. Song, Y. Chi, *Chem. Commun.* **2003**, 2628–2629; b) H.-Y. Chen, Y. Chi, C.-S. Liu, J.-K. Yu, Y.-M. Cheng, K.-S. Chen, P.-T. Chou, S.-M. Peng, G.-H. Lee, A. J. Carty, S.-J. Yeh, C.-T. Chen, *Adv. Funct. Mater.* **2005**, *15*, 567–574.

[10] a) Q. Zhang, J. Li, K. Shizu, S. Huang, S. Hirata, H. Miyazaki, C. Adachi, *J. Am. Chem. Soc.* **2012**, *134*, 14706–14709; b) S. Wu, M. Aonuma, Q. Zhang, S. Huang, T. Nakagawa, K. Kuwabara, C. Adachi, *J. Mater. Chem. C* **2014**, *2*, 421–424; c) K. Albrecht, K. Matsuoka, K. Fujita, K. Yamamoto, *Angew. Chem. Int. Ed.* **2015**, *54*, 5677–5682; *Angew. Chem.* **2015**, *127*, 5769–5774.

[11] A. Bigot, D. Breuninger, B. Breit, *Org. Lett.* **2008**, *10*, 5321–5324.

[12] a) S. Wang, *Coord. Chem. Rev.* **2001**, *215*, 79–98; b) Y. Sun, N. Ross, S.-B. Zhao, K. Huszarik, W.-L. Jia, R.-Y. Wang, D. Macartney, S. Wang, *J. Am. Chem. Soc.* **2007**, *129*, 7510–7511; c) Z. M. Hudson, S. Wang, *Acc. Chem. Res.* **2009**, *42*, 1584–1596.

[13] a) A. Marini, A. Muñoz-Losa, A. Biancardi, B. Mennucci, *J. Phys. Chem. B* **2010**, *114*, 17128–17135; b) K.-Y. Liao, C.-W. Hsu, Y. Chi, M.-K. Hsu, S.-W. Wu, C.-H. Chang, S.-H. Liu, G.-H. Lee, P.-T. Chou, Y. Hu, N. Robertson, *Inorg. Chem.* **2015**, *54*, 4029–4038.

[14] S. Huang, Q. Zhang, Y. Shiota, T. Nakagawa, K. Kuwabara, K. Yoshizawa, C. Adachi, *J. Chem. Theory Comput.* **2013**, *9*, 3872–3877.

[15] a) J. Wu, W. Liu, J. Ge, H. Zhang, P. Wang, *Chem. Soc. Rev.* **2011**, *40*, 3483–3495; b) Y. Kubota, Y. Sakuma, K. Funabiki, M. Matsui, *J. Phys. Chem. A* **2014**, *118*, 8717–8729.

[16] J. Lee, K. Shizu, H. Tanaka, H. Nakanotani, T. Yasuda, H. Kaji, C. Adachi, *J. Mater. Chem. C* **2015**, *3*, 2175–2181.

[17] J. R. Kirchhoff, R. E. Gamache, M. W. Blaskie, A. A. Del Paggio, R. K. Lengel, D. R. McMillin, *Inorg. Chem.* **1983**, *22*, 2380–2384.

[18] a) S.-J. Su, E. Gonmori, H. Sasabe, J. Kido, *Adv. Mater.* **2008**, *20*, 4189–4194; b) Y.-Y. Lyu, J. Kwak, W. S. Jeon, Y. Byun, H. S. Lee, D. Kim, C. Lee, K. Char, *Adv. Funct. Mater.* **2009**, *19*, 420–427.

[19] C. C. Wu, Y. T. Lin, K. T. Wong, R. T. Chen, Y. Y. Chien, *Adv. Mater.* **2004**, *16*, 61–65.

[20] L. Xiao, Z. Chen, B. Qu, J. Luo, S. Kong, Q. Gong, J. Kido, *Adv. Mater.* **2011**, *23*, 926–952.